

PAPER

## Setting the stage for materials simulation using acoustic metamaterials digital quantum analogue computing platforms

To cite this article: P A Deymier *et al* 2022 *Modelling Simul. Mater. Sci. Eng.* **30** 084003

View the [article online](#) for updates and enhancements.

### You may also like

- [Standard model physics and the digital quantum revolution: thoughts about the interface](#)  
Natalie Klco, Alessandro Roggero and Martin J Savage
- [Quantum information processing with superconducting circuits: a review](#)  
G Wendin
- [Quantum computer-aided design of quantum optics hardware](#)  
Jakob S Kottmann, Mario Krenn, Thi Ha Kyaw *et al.*





**IOP | ebooks™**

Bringing together innovative digital publishing with leading authors from the global scientific community.

Start exploring the collection—download the first chapter of every title for free.

# Setting the stage for materials simulation using acoustic metamaterials digital quantum analogue computing platforms

P A Deymier<sup>1,\*</sup> , K Runge<sup>1</sup>, M A Hasan<sup>2</sup> , J A Levine<sup>3</sup> and P Cutillas<sup>4</sup>

<sup>1</sup> Department of Materials Science and Engineering, University of Arizona, Tucson, AZ 85721, United States of America

<sup>2</sup> Department of Mechanical Engineering, Wayne State University, Detroit, MI 48202, United States of America

<sup>3</sup> Department of Computer Science, The University of Arizona, Tucson, AZ 85721, United States of America

<sup>4</sup> Department of Computer Science, University of Southern California, Los Angeles, CA 90089, United States of America

E-mail: [deymier@arizona.edu](mailto:deymier@arizona.edu)

Received 7 June 2022; revised 12 September 2022

Accepted for publication 11 October 2022

Published 20 October 2022



CrossMark

## Abstract

We present a model of an externally driven acoustic metamaterial constituted of a nonlinear parallel array of coupled acoustic waveguides that supports logical phi-bits, classical analogues of quantum bits (qubit). Descriptions of correlated multiple phi-bit systems emphasize the importance of representations of phi-bit and multiple phi-bit vector states within the context of their corresponding Hilbert space. Experimental data are used to demonstrate the realization of the single phi-bit Hadamard gate and the phase shift gate. A three phi-bit system is also used to illustrate the development of multiple phi-bit gates as well as a simple quantum-like algorithm. These demonstrations set the stage for the implementation of a digital quantum analogue computing platform based on acoustic metamaterial that can implement quantum-like gates and may offer promise as an efficient platform for the simulation of materials.

**Keywords:** acoustic metamaterial, digital quantum analogue computer, materials simulation

(Some figures may appear in colour only in the online journal)

\* Author to whom any correspondence should be addressed.

## 1. Introduction

Digital quantum computers are starting to provide efficient platforms for the simulation of materials and in particular quantum materials [1–4]. Digital quantum computers are constituted of a set of quantum bits (qubits) on which one can operate through a universal set of quantum logic gates. These gates are reversible unitary operations that act on a state or a superposition of states of qubits producing a predictable and eventually measurable output. Any operation can be expressed as a finite sequence of gates forming a set of universal quantum gates [5]. Among such logic gates are the single qubit Hadamard gate and the phase shift gate. Examples of two qubit logic gates include the controlled NOT (CNOT) gate. Here, we focus on digital computing platforms in contrast to quantum simulators which exploit the isomorphism between the Hamiltonian of the simulator and that of the quantum system to be simulated [6].

The advantage of qubits over conventional bits results from their quantum wave functions which are probability amplitudes and can support coherent superpositions of states. For instance, the state of a single qubit can be in a superposition of state  $\psi = \alpha|0\rangle + \beta|1\rangle$ . Here, the kets  $|0\rangle$  and  $|1\rangle$  form the basis for expanding the wave function  $\psi$ . The coefficients  $\alpha$  and  $\beta$  are complex quantities. The wave function  $\psi$  can therefore be represented as a complex state vector in a Hilbert space whose basis is  $\{|0\rangle, |1\rangle\}$  with components  $\alpha$  and  $\beta$ . Coherence results from the phase relation between these two coefficients. Unitary operations on a single qubit are effectively rotations of the state vector in the Hilbert space. The wave function of a two partite quantum system composed of two qubits can also be represented as a vector in a  $2^2$ -dimensional Hilbert space tensor product of the 2D Hilbert spaces of the constitutive qubits. The basis vectors of the composite Hilbert space  $\{|0\rangle|0\rangle, |0\rangle|1\rangle, |1\rangle|0\rangle, |1\rangle|1\rangle\}$  are tensor products of the basis vectors of the individual qubits. The components of the two-qubit state vector are phase related and the two qubits wave function forms a coherent superposition. Unitary operations on two qubit wave functions are rotations in their 4D Hilbert space. This concept easily generalizes to  $N > 2$  qubits with their Hilbert space scaling exponentially as  $2^N$ . Quantum computing is therefore essentially a phase computing approach; it exploits the possibility of realizing and rotating coherent superpositions of states of multipartite systems with complex amplitudes that are represented as vectors in large exponentially scaling Hilbert spaces. In the Hilbert space of multipartite quantum systems, some vector states cannot be factored into tensor products of subsystems composed of small number of qubits. These states are said to be non-separable. Non-separability is at the core of quantum entanglement, a form of quantum correlation leading to the interdependency of states of individual qubits in a multipartite system. This leads to the parallelism of quantum computing since an operation affecting one qubit may then affect all other qubits simultaneously. However, since the quantum wave function is a probability amplitude, quantum computing with multiple qubits suffers from the fragility of quantum superpositions of states against perturbations or undesired interactions, i.e. it suffers from the collapse of the wave function upon a perturbation such as a measurement. To overcome the drawback of qubits in quantum computing, we have recently introduced the notion of ‘logical phi-bit’ [7]. A logical phi-bit is a two-state degree of freedom of a nonlinear acoustic wave supported by a metamaterial, which can be in a coherent superposition of states with complex amplitude coefficients and hence realizes a qubit classical analogue. The wave function of a logical phi-bit is an amplitude and does not suffer from quantum fragility. We have demonstrated experimentally the exponential complexity and scalability of the Hilbert space of states of multiple phi-bits and also the non-separability of coherent superpositions to reveal their applicability to quantum information science [7]. Since the CNOT gate is one of the keys to unlock the power of quantum computing, we

demonstrated experimentally the systematic and predictable operation of a two phi-bit CNOT gate [8].

In this paper, we present a model of an externally driven acoustic metamaterial constituted of a nonlinear parallel array of coupled acoustic waveguides that supports logical phi-bits. We describe a logical phi-bit as a two-level system with complex amplitudes analogous to a qubit. We also unravel the correlations between phi-bits and the description of multiple phi-bit systems within the context of exponentially scaling Hilbert spaces. We also emphasize the importance of representation of phi-bit and multiple phi-bit vector states as the result of changes in the Hilbert space basis. Experimental data are used to demonstrate the effect of representations in the realization of the single phi-bit Hadamard gate and the phase shift gate. A three phi-bit system is also used to illustrate the development of multiple phi-bit gates as well as a simple quantum-like algorithm. This work sets the stage for the implementation of a digital quantum analogue computing platform based on acoustic metamaterial that can implement quantum-like gates and may offer promise as an efficient platform for the simulation of materials.

## 2. Model of acoustic metamaterials quantum analogue computing platform

### 2.1. Logical Phi-bit in nonlinearly coupled array of elastic waveguides

The acoustic metamaterial is composed of three one-dimensional (1D) elastic waveguides coupled elastically along their length (figure 1). Each waveguide is driven externally at its end at the position  $x = 0$ .  $x$  represents the position along the waveguides.

The nonlinear elastic wave equation in the long wavelength limit is given by:

$$\left[ \left( \frac{\partial^2}{\partial t^2} - \beta^2 \frac{\partial^2}{\partial x^2} + \mu \frac{\partial}{\partial t} \right) \vec{I} + \alpha^2 \vec{M} \right] \vec{U} + \varepsilon \vec{G}(\vec{U}) = \vec{F}_1 \delta_{x=0} \cos \omega_1 t + \vec{F}_2 \delta_{x=0} \cos \omega_2 t. \quad (1)$$

The parameter  $\beta$  is proportional to the speed of sound along the waveguides. The parameter  $\mu$  represents damping.  $\vec{I}$  is the identity matrix.  $\alpha$  measures the elastic coupling strength between waveguides.  $\vec{M}$  is the matrix characterizing the elastic coupling between the three waveguides. In the case of a planar array of waveguides, the coupling matrix takes the form:

$$\vec{M} = \begin{pmatrix} 1 & -1 & 0 \\ -1 & 2 & -1 \\ 0 & -1 & 1 \end{pmatrix} \quad (2)$$

where  $\vec{F}_1$  and  $\vec{F}_2$  are  $3 \times 1$  vectors representing the external driving harmonic forces for two different driving angular frequencies  $\omega_1 = 2\pi f_1$  and  $\omega_2 = 2\pi f_2$ .

The displacement in waveguides 1, 2 and 3 is represented by the  $3 \times 1$  vector  $\vec{U} = (U_1, U_2, U_3)$ .  $\varepsilon \vec{G}(\vec{U})$  is a nonlinear term with strength  $\varepsilon$ . In this model we consider a simple quadratic nonlinearity which depends on the difference in the displacement between adjacent waveguides:

$$\vec{G}(\vec{U}) = \begin{pmatrix} (U_1 - U_2)^2 \\ - (U_1 - U_2)^2 + (U_2 - U_3)^2 \\ - (U_2 - U_3)^2 \end{pmatrix}. \quad (3)$$

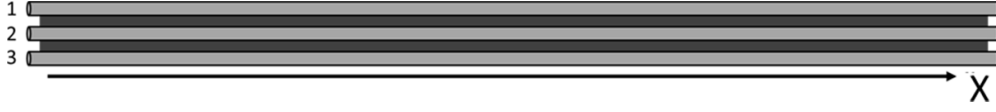


**Figure 1.** Schematic of the metamaterial composed of a parallel array of three coupled waveguides.

To solve equation (1) we use perturbation theory. For small  $\varepsilon$ , the displacement field is initially expanded to first order in perturbation:

$$U = \vec{U}^{(0)} + \varepsilon \vec{U}^{(1)}. \quad (4)$$

This expansion yields equation (1) to zeroth order:

$$\left[ \left( \frac{\partial^2}{\partial t^2} - \beta^2 \frac{\partial^2}{\partial x^2} + \mu \frac{\partial}{\partial t} \right) \vec{I} + \alpha^2 \vec{M} \right] \vec{U}^{(0)} = \vec{F}_1 \delta_{x=0} e^{i\omega_1 t} + \vec{F}_2 \delta_{x=0} e^{i\omega_2 t}. \quad (5)$$

We can solve this equation by defining by  $\lambda_n$  and  $\vec{E}_n$  with  $n = 1, 2, 3$ , the eigen values and eigen vectors of the  $\vec{M}$  matrix, where  $\vec{E}_n$  represent the spatial eigen modes across the waveguides with components  $E_{n,j}$ ,  $j = 1, 2, 3$ . We write:

$$\vec{M} \vec{E}_n = \lambda_n \vec{I} \vec{E}_n. \quad (6)$$

The first eigen vector for which  $\lambda_1 = 0$ , is  $\vec{E}_{11}^T = \frac{1}{\sqrt{3}} (1, 1, 1)$ . The other two eigen modes have eigen values  $\lambda_2 = 1$ , and  $\lambda_3 = 3$ , and are given by:

$$\vec{E}_2 = \begin{pmatrix} E_{2,1} \\ E_{2,2} \\ E_{2,3} \end{pmatrix} = \frac{1}{\sqrt{2}} \begin{pmatrix} 1 \\ 0 \\ -1 \end{pmatrix}, \vec{E}_3 = \begin{pmatrix} E_{3,1} \\ E_{3,2} \\ E_{3,3} \end{pmatrix} = \frac{1}{\sqrt{6}} \begin{pmatrix} 1 \\ -2 \\ 1 \end{pmatrix}.$$

We can now expand the displacement vector on the complete orthonormal basis,  $\{\vec{E}_n\}$ :

$$\vec{U}^{(0)} = \sum_n u_n^{(0)} \vec{E}_n. \quad (7)$$

Since equation (5) is linear, we focus on an external force with a single driving frequency,  $\vec{F}_l$  with  $l = 1$  or  $2$ . We seek solutions of the simplified equation:

$$\left[ \left( \frac{\partial^2}{\partial t^2} - \beta^2 \frac{\partial^2}{\partial x^2} + \mu \frac{\partial}{\partial t} \right) \vec{I} + \alpha^2 \vec{M} \right] \vec{U}_l^{(0)} = \vec{F}_l \delta_{x=0} e^{i\omega_l t}. \quad (8)$$

The  $3 \times 1$  vector,  $\vec{F}_l$ , is also expanded on the basis  $\{\vec{E}_n\}$ :

$$\vec{F}_l = \sum_n F_n^{(l)} \vec{E}_n. \quad (9)$$

Inserting equations (6)–(8) into equation (5) yields a set of three equations of the form:

$$\left( \frac{\partial^2}{\partial t^2} - \beta^2 \frac{\partial^2}{\partial x^2} + \mu \frac{\partial}{\partial t} + \alpha^2 \lambda_n \right) u_{n,l}^{(0)} = F_n^{(l)} \delta_{x=0} e^{i\omega_l t}. \quad (10)$$

The coefficients  $u_{n,l}^{(0)}$  are now expanded on plane waves which follow the harmonic driving force:

$$u_{n,l}^{(0)} = \sum_{k_n} A_{n,l}(k_n) e^{ik_n x} e^{i\omega_l t}. \quad (11)$$

Since the waveguides are finite in length, the wave numbers,  $k_n$ , form a discrete set. Equation (10) is now evaluated at  $x = 0$  leading to the driven complex amplitudes:

$$A_{n,l}(k_n) = \frac{F_n^{(l)}}{\omega_{0,n}^2(k_n) - \omega_l^2 + i\mu\omega_l} \quad (12)$$

where we define the characteristic frequency

$$\omega_{0,n}^2(k_n) = \beta^2 k_n^2 + \alpha^2 \lambda_n. \quad (13)$$

To zeroth order the displacement field is found to be

$$\vec{U}_l^{(0)} = \sum_{n=1}^3 \vec{E}_n \sum_{k_n} A_{n,l}(k_n) e^{ik_n x} e^{i\omega_l t} \quad (14)$$

with the complex resonant amplitudes given by equation (12). We note that these amplitudes are complex quantities as a result of the dissipative term  $i\mu\omega$ . Rewriting the linear displacement field for driving forces with two different frequencies, one gets:

$$\begin{aligned} \vec{U}^{(0)} &= \vec{U}_1^{(0)} + \vec{U}_2^{(0)} \\ &= \sum_{n=1}^3 \vec{E}_n \left( \sum_{k_n} A_{n,1}(k_n) e^{ik_n x} e^{i\omega_1 t} + \sum_{k'_n} A_{n,2}(k'_n) e^{ik'_n x} e^{i\omega_2 t} \right). \end{aligned} \quad (15)$$

Here, we have used two independent summation indices for the wavenumber, namely  $k_n$  and  $k'_n$ .

Now that we have the linear displacement field, we can solve the wave equation to first order in perturbation since the zeroth order displacement drives the system with mixed frequencies.

This equation takes the form:

$$\left[ \left( \frac{\partial^2}{\partial t^2} - \beta^2 \frac{\partial^2}{\partial x^2} + \mu \frac{\partial}{\partial t} \right) \vec{I} + \alpha^2 \vec{M} \right] \vec{U}^{(1)} + \vec{G}(\vec{U}^{(0)}) = 0. \quad (16)$$

Let us introduce the quantities  $S_{n,l} = \sum_{k_n} A_{n,l}(k_n) e^{ik_n x}$ . The first component of the quadratic nonlinear term is:

$$\left\{ \left( U_1^{(0)} - U_2^{(0)} \right)^2 \right\}_{\omega_1, \omega_2} = \left( \sum_{n=1}^3 (E_{n,1} - E_{n,2}) \left( S_{n,l=1} e^{i\omega_1 t} + S_{n,l=2} e^{i\omega_2 t} \right) \right)^2. \quad (17)$$

We focus on the terms which mix the two different frequencies and reduce equation (17) to

$$\left( U_1^{(0)} - U_2^{(0)} \right)^2 = \sum_{n=1}^3 \sum_{m=1}^3 g_{n,m}^{1,2} S_{n,l=1} S_{m,l=2} e^{i(\omega_1 + \omega_2)t} \quad (18)$$

where  $g_{n,m}^{1,2} = 2(E_{n,1} - E_{n,2})(E_{m,1} - E_{m,2})$ .

In equation (18), there are nine  $\{n, m\}$  terms contributing to  $\vec{G}(\vec{U}^{(0)})$  taking the form of  $3 \times 1$  vectors  $\begin{pmatrix} g_{n,m}^{1,2} \\ -g_{n,m}^{1,2} + g_{n,m}^{2,3} \\ -g_{n,m}^{2,3} \end{pmatrix}$ . Each of these vectors can be expanded on the complete basis  $\{\vec{E}_n\}$  in the form  $\sum_p \tilde{g}_p^{(n,m)} \vec{E}_p$ .

This allows use to express the nonlinear term as:

$$\vec{G}(\vec{U}^{(0)}) = \sum_p \sum_{n=1}^3 \sum_{m=1}^3 \tilde{g}_p^{(n,m)} \vec{E}_p S_{n,l=1} S_{m,l=2} e^{i(\omega_1 + \omega_2)t}. \quad (19)$$

Similarly, we also expand the first order displacement field for each  $\{n, m\}$  term on  $\{\vec{E}_n\}$ :  $\vec{U}^{(1)}(n, m) = \sum_p u_p^{(1)}(n, m) \vec{E}_p$ , enabling us to write:

$$\vec{U}^{(1)} = \sum_p \sum_{n=1}^3 \sum_{m=1}^3 u_p^{(1)}(n, m) \vec{E}_p S_{n,l=1} S_{m,l=2} e^{i(\omega_1 + \omega_2)t}. \quad (20)$$

Inserting these expansions into equation (16), the first order equations of motion reduce to three equations with  $p = 1, 2, 3$ :

$$\left( -i(\omega_1 + \omega_2)^2 + \beta^2(k_n + k_m)^2 + i\mu(\omega_1 + \omega_2) + \alpha^2\lambda_p \right) u_p^{(1)}(n, m) + \tilde{g}_p^{(n,m)} = 0 \quad (21)$$

which yield the complex resonant amplitudes

$$u_p^{(1)}(n, m) = \frac{-\tilde{g}_p^{(n,m)}}{\left( -(\omega_1 + \omega_2)^2 + \beta^2(k_n + k_m)^2 + i\mu(\omega_1 + \omega_2) + \alpha^2\lambda_p \right)}. \quad (22)$$

The complete nonlinear first order displacement field for the sum of frequencies  $\omega_1 + \omega_2$  evaluated at one end of the waveguide array (say  $x = 0$ ), reads

$$\vec{U}^{(1)} = \sum_p \sum_{n=1}^3 \sum_{m=1}^3 u_p^{(1)}(n, m) \vec{E}_p \sum_{k_n} \sum_{k_m} A_{n,1}(k_n) A_{m,2}(k_m) e^{i(\omega_1 + \omega_2)t}. \quad (23)$$

The nonlinear displacement is a coherent superposition of states in the basis  $\{\vec{E}_n\}$  with complex coefficients. These coefficients are product of Lorentzian-type resonances.

This displacement field can be expressed in the compact form:

$$\vec{U}^{(1)} = \begin{pmatrix} C_1 e^{i\varphi_1} \\ C_2 e^{i\varphi_2} \\ C_3 e^{i\varphi_3} \end{pmatrix} e^{i(\omega_1 + \omega_2)t}. \quad (24)$$

The phases  $\varphi_1$ ,  $\varphi_2$  and  $\varphi_3$  arise from the complex nature of the resonant amplitudes,  $u_p^{(1)}(n, m)$ ,  $A_{n,1}(k_n)$  and  $A_{m,2}(k_m)$ . Equation (24) can be reformulated by normalization and considering two phase differences only:

$$\vec{U}^{(1)} = \begin{pmatrix} 1 \\ \hat{C}_2 e^{i\varphi_{12}} \\ \hat{C}_3 e^{i\varphi_{13}} \end{pmatrix} e^{i(\omega_1 + \omega_2)t} \quad (25)$$

where  $\hat{C}_2$  and  $\hat{C}_3$  are normalized to  $C_1$  and  $\varphi_{12} = \varphi_2 - \varphi_1$  and  $\varphi_{13} = \varphi_3 - \varphi_1$ . We reduce this expression by dropping direct reference to waveguide 1. We now define the displacement field at the end of the waveguides by the renormalized  $2 \times 1$  vector:

$$\vec{U}^{(1)} = \begin{pmatrix} \hat{c}_2 e^{i\varphi_{12}} \\ \hat{c}_3 e^{i\varphi_{13}} \end{pmatrix} e^{i(\omega_1 + \omega_2)t}. \quad (26)$$

The mixed frequency,  $\omega_1 + \omega_2$ , serves as a good quantum number for defining a logical phi-bit. A logical phi-bit in a nonlinear acoustic metamaterial composed of coupled 1D waveguides is defined as a two-state degree of freedom of an elastic wave, which can be in a coherent superposition of states with complex amplitude coefficients. Phi-bit states live on the Bloch sphere. A logical phi-bit is therefore a classical analogue of a qubit—the critical component of quantum computing platforms.

## 2.2. Generalized logical phi-bit—second order solution

In order to illustrate other logical phi-bits in the form of nonlinear modes, we consider the expansion of the displacement field to second order in perturbation:

$$\vec{U} = \vec{U}^{(0)} + \varepsilon \vec{U}^{(1)} + \varepsilon^2 \vec{U}^{(2)}. \quad (27)$$

The second order equation takes the form:

$$\left[ \left( \frac{\partial^2}{\partial t^2} - \beta^2 \frac{\partial^2}{\partial x^2} + \mu \frac{\partial}{\partial t} \right) \vec{I} + \alpha^2 \vec{M} \right] \vec{U}^{(2)} + \vec{G}(\vec{U}^{(0)}, \vec{U}^{(1)}) = 0 \quad (28)$$

where the components of  $\vec{G}(\vec{U}^{(0)}, \vec{U}^{(1)})$  are given by

$$\begin{pmatrix} 2(U_1^{(0)} - U_2^{(0)})(U_1^{(1)} - U_2^{(1)}) \\ -2(U_1^{(0)} - U_2^{(0)})(U_1^{(1)} - U_2^{(1)}) - 2(U_2^{(0)} - U_3^{(0)})(U_2^{(1)} - U_3^{(1)}) \\ 2(U_2^{(0)} - U_3^{(0)})(U_2^{(1)} - U_3^{(1)}) \end{pmatrix}. \quad (29)$$

The zeroth and first order solution drive the second order equation (28). Some solutions of equation (28) will have mixed frequencies of the type  $2\omega_1 + \omega_2$  or  $\omega_1 + 2\omega_2$  and will constitute additional logical phi-bits. Even higher order solutions or solutions of the wave equation with nonlinearity going beyond the quadratic character discussed so far will produce logical phi-bits. These logical phi-bits will appear as nonlinear peaks in the Fourier spectrum of the displacement field of the coupled waveguide system. We therefore represent logical phi-bits in the generalized form of a  $2 \times 1$  vector characterizing the displacement field at the end of the waveguides by:

$$\vec{U}_{(i)} = \begin{pmatrix} \hat{c}_2 e^{i\varphi_{12}} \\ \hat{c}_3 e^{i\varphi_{13}} \end{pmatrix} e^{i\omega^{(i)}t} \quad (29)$$

where  $\hat{c}_2$  and  $\hat{c}_3$  are normalized amplitudes and all phases are referred to that of the waveguide 1.  $\omega^{(i)} = (s\omega_1 + t\omega_2)$  where  $s$  and  $t$  are integers, is the frequency of a nonlinear mode, ‘ $i$ ’, mixing the two drivers’ frequencies  $\omega_1$  and  $\omega_2$ . Note that the complex amplitudes  $\hat{c}_2$  and  $\hat{c}_3$  of a given phi-bit are linear combination of products of resonant amplitudes of zeroth order solutions or other nonlinear modes. The complex amplitudes of phi-bits with different quantum numbers  $\omega^{(i)}$  are therefore phase locked. That is, there exist a phase relation between the complex amplitudes of different phi-bits coexisting within the metamaterial. Logical phi-bits are subsequently correlated through these phase relations. The representation



of the nonlinear mode given by equation (29) is expressed in the space of the waveguides. That is, the  $2 \times 1$  amplitude is represented on a basis  $\left\{ \begin{pmatrix} 1 \\ 0 \end{pmatrix}, \begin{pmatrix} 0 \\ 1 \end{pmatrix} \right\}$  which orthogonal unit vectors correspond to waveguides 2 and 3, respectively.

### 2.3. Multiple phi-bit systems and their representations

A logical phi-bit with frequency  $\omega^{(i)}$  is effectively an oscillator. An equation of motion representing the evolution of oscillations along the positive timeline of a phi-bit oscillator may be constructed in the form:

$$\left[ \left( -\frac{d}{dt} + i\omega^{(i)} \right) \vec{I}_{2 \times 2} + \vec{C}_{2 \times 2}^{(i)} \right] \vec{V}_{(i)} = 0. \quad (30)$$

When we define a solution as  $\vec{V}_{(i)} = \begin{pmatrix} V_1^{(i)} \\ V_2^{(i)} \end{pmatrix} e^{i\omega^{(i)}t}$ , one recovers the single phi-bit representation given by equation (29) when  $\vec{C}_{2 \times 2}^{(i)} = \begin{pmatrix} -1 & X \\ -X^{-1} & 1 \end{pmatrix}$  with  $X = \hat{c}_2 e^{i\varphi_{12}} / \hat{c}_3 e^{i\varphi_{13}}$ . The eigen values of the matrix  $\vec{C}_{2 \times 2}^{(i)}$  are equal to zero and the eigen frequency  $\omega^{(i)}$  is equal to the characteristic frequency of the oscillator,  $\omega^{(i)}$ . The product of functions  $e^{i\omega^{(i)}t}$  and the eigen vectors of  $\vec{C}_{2 \times 2}^{(i)}$  form a complete basis for the states of a phi-bit oscillator, 'i' thus defining the Hilbert space,  $h_{(i)}$ , of a single phi-bit.

The equations of motion for a multipartite system composed of  $N$  independent phi-bits may take the form:

$$\left[ \left( -\frac{d}{dt} + i\omega^{(1)} + \dots + i\omega^{(N)} \right) \vec{I}_{2^N \times 2^N} + \vec{C}_{2 \times 2}^{(1)} \otimes \dots \otimes \vec{C}_{2 \times 2}^{(N)} \right] \vec{W} = 0. \quad (31)$$

Which solutions are tensor products of single phi-bit states and given by:  $\vec{W} = \vec{U}_{(1)} \otimes \dots \otimes \vec{U}_{(N)}$ . Consequently, the tensor product of the basis vectors of single phi-bit forms a complete basis for the states of the non-interacting multiple phi-bit system. This basis describes vector states in a  $2^N$  dimensional Hilbert space,  $H$ . This space is the tensor product of the  $N$  Hilbert spaces of the individual phi-bits,  $H = h_{(1)} \otimes \dots \otimes h_{(N)}$ . When the phi-bits interact, the tensor product  $\vec{C}_{2 \times 2}^{(1)} \otimes \dots \otimes \vec{C}_{2 \times 2}^{(N)}$  in equation (31) is replaced by a general matrix operator  $\vec{C}_{2^N \times 2^N}$ . However, the Hilbert space spanned by the states of the interacting phi-bit system is the same as that of the non-interacting phi-bits. A vector state of the interacting phi-bits can then be written as a linear combination of the basis vectors of  $H$ . The coefficient of this superposition of states are complex quantities. A given set of basis vectors in the system's Hilbert space corresponds to but one of the many possible representations of the  $N$  phi-bit system.

Different representations of the  $N$  phi-bit system can be realized by applying a unitary transformation to the basis of  $H$ . This is equivalent to a change of coordinate system. It is not necessary to know the unitary transformation to define a new representation of the multiple phi-bit system. In the subsequent sections, we will construct different representation of phi-bits under the assumption that one can eventually find the corresponding unitary transformation.

We also note that the components of a  $2^N$  dimensional state vector of a multiple logical phi-bit system are correlated. Physical manipulation of a metamaterial supporting  $N$  logical phi-bits will result in a rotation in the system's Hilbert space. The components of the system's state vector will change simultaneously in a manner prescribed by their physical phase relations.

The simultaneous change of the components of the state vector in an exponentially complex Hilbert space offers promise in achieving massively parallel processing capabilities.

### 3. Experimental validation of acoustic metamaterial operations

In the next section, we validate experimentally some specific and universal operations on examples of logical phi-bit systems. The physical metamaterial is composed of an array of three elastically coupled acoustic waveguides that produces a nonlinear displacement field which can be partitioned in the frequency domain [7]. Each waveguide consists of a finite length aluminum rod with circular cross section. The rods are arranged in a linear array with a lateral gap filled with epoxy. Ultrasonic transducers drive and detect the acoustic field at the ends of the rods. Function generators and amplifiers are used to excite two driving transducers attached to the ends of guide 1 and 2 with sinusoidal signals of same magnitude but with frequency  $f_1 = 62$  kHz,  $f_2 = 66$  kHz. These frequencies were selected for illustrative purpose. Experiments conducted with other frequencies showed qualitatively similar behavior. The driving frequency of the first rod is modified according to  $f_1 = 62$  kHz  $- \Delta v$  where the tuning parameter  $\Delta v$  is used to navigate the logical phi-bits Hilbert space. Three detecting transducers located at the opposite ends of the rods collect data on the displacement field. The nonlinearity of this driven system leads to many ways of mixing the drivers' frequencies as was discussed in section 2.2. The measured displacement field at the detection end of the waveguides is the Fourier sum of a large number of linear and nonlinear modes, each with its own characteristic frequency. That is, each one of these nonlinear modes appearing as peaks in the Fourier spectrum of the displacement field is effectively a logical phi-bit. Additional details on this physical system can be found in [7]. Briefly, in the experiment, the oscilloscope records the driving and response signals, which are averaged over 128 time series. We conducted numerous sets of independent experimental measurements and found that the phase had an estimated experimental uncertainty of less than  $\pi/9$ . In addition, because the force transducers are not bonded to the sample, the layer of couplant on the sample's edges was kept constant throughout the experiments by maintaining a constant pressure on the transducers.

#### 3.1. Hadamard gate operation on a single logical phi-bit

Here, we focus our attention on a single phi-bit (nonlinear mode) in the Fourier spectrum of the displacement field with frequency  $f_1 - \Delta f$  with  $\Delta f = |f_2 - f_1|$ . (i.e.  $2f_1 - f_2$ ). The phases  $\varphi_{12}$  and  $\varphi_{13}$  as functions of tuning parameter  $\Delta v \in [0, 4000]$  Hz in increments of 10 Hz are reported in figure 2(a). We change the  $2 \times 1$  vector representation of this phi-bit amplitude from that of equation (3) to another representation defined as  $\vec{U}' = \begin{pmatrix} \cos \Delta \varphi \\ \sin \Delta \varphi \end{pmatrix} = \begin{pmatrix} \cos S [(\varphi_{12} - \varphi_{12}^0) - (\varphi_{13} - \varphi_{13}^0)] \\ \sin S [(\varphi_{12} - \varphi_{12}^0) - (\varphi_{13} - \varphi_{13}^0)] \end{pmatrix}$  where  $\varphi_{12}^0 = \varphi_{12}(\Delta v = 0)$  and  $\varphi_{13}^0 = \varphi_{13}(\Delta v = 0)$  and the factor  $S$  scales the phase difference to  $2\pi$ . This representation limits the components of  $\vec{U}'$  to real number. The components of this amplitude vector as a function of tuning parameter are presented in figure 2(b).

Figure 2(b) shows that the two components of  $\vec{U}'$  vary simultaneously and coherently with the tuning parameter. It also shows that with a proper choice of the tuning parameter one can realize a number of pure states and superpositions of states and relate them through a unitary transformation similar to the Hadamard gate matrix:  $H_a = \frac{1}{\sqrt{2}} \begin{pmatrix} 1 & 1 \\ 1 & -1 \end{pmatrix}$ . Some of

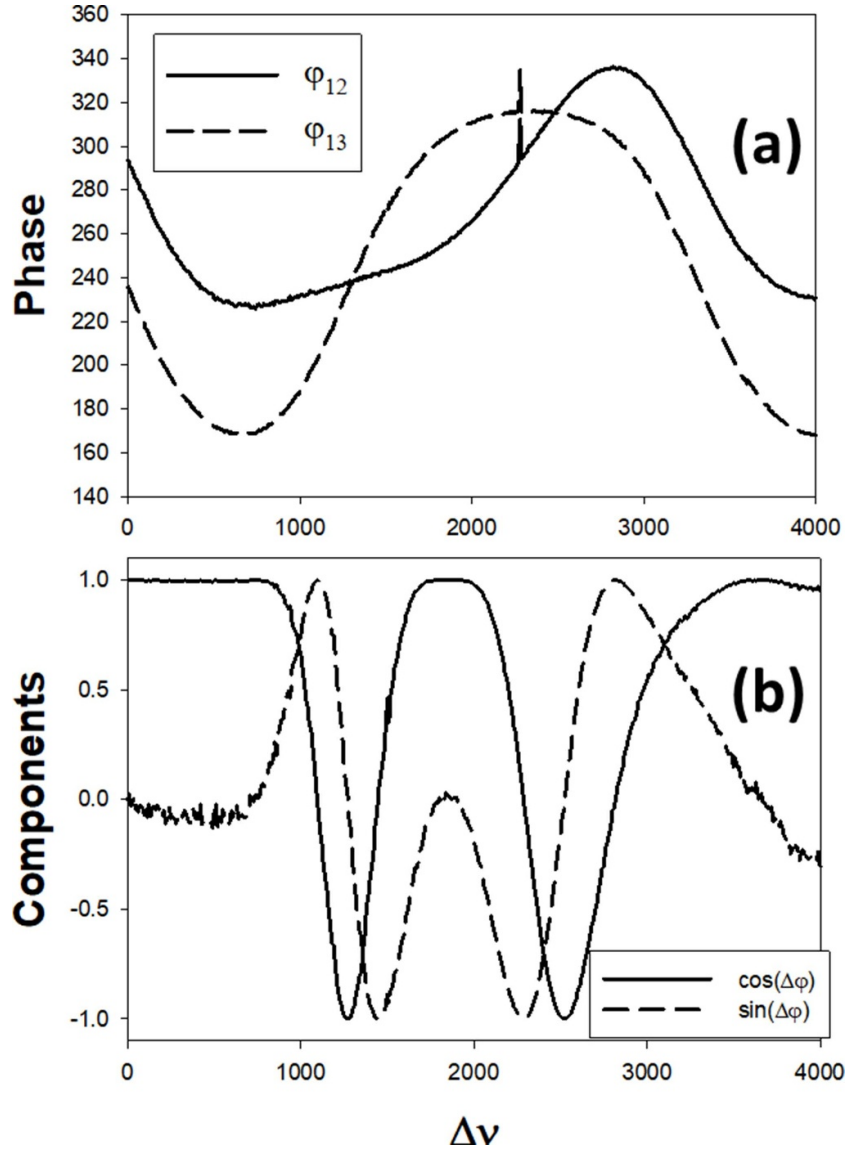


**Figure 2.** Phi-bit with frequency  $2f_1 - f_2$ . (a) Phases  $\varphi_{12}$  and  $\varphi_{13}$  as functions of driving frequency tuning parameter  $\Delta\nu$ . (b) Components of the  $\vec{U}'$  representation of the phi-bit state (see text for details) as function of tuning parameter.

these states with their associated value of the tuning parameter are summarized in table 1. The Hadamard gate operation that takes a pure state  $\begin{pmatrix} 1 \\ 0 \end{pmatrix}$  or  $\begin{pmatrix} 0 \\ 1 \end{pmatrix}$  into the coherent superpositions of states  $\begin{pmatrix} 1 \\ 1 \end{pmatrix}$  or  $\begin{pmatrix} 1 \\ -1 \end{pmatrix}$  can then be implemented by applying physically a systematic and predictable change of 200 Hz in the value of the tuning parameter.

**Table 1.** Examples of values of the tuning parameter  $\Delta v$  realizing  $\vec{U}'$  states with real components related to within a general phase of 0 or  $\pi$  by the Hadamard gate,  $H_a$ . Note that the states in this table may not be normalized.

$\Delta v$ (Hz)	780	980	1100	1300
State	$\begin{pmatrix} 1 \\ 0 \end{pmatrix}$	$\begin{pmatrix} 1 \\ 1 \end{pmatrix}$	$\begin{pmatrix} 0 \\ 1 \end{pmatrix}$	$-\begin{pmatrix} 1 \\ -1 \end{pmatrix}$
Operation	$H_a \equiv \delta(\Delta v) = 200 \text{ Hz}$		$H_a \equiv \delta(\Delta v) = 200 \text{ Hz}$	

So far, the Hadamard gate realized here is an initial illustration of the potential of logical phi-bits for quantum analogue computing. Representations of phi-bit states with complex coefficients and the capability to manipulate the relative phase between these coefficients is described in the next subsection.

### 3.2. Phase gate

The phase shift gate or phase gate is a single phi-bit gate that keeps one component of a phi-bit representation constant and phase shifts the other component. The gate matrix representation is  $P(\varphi) = \begin{pmatrix} 1 & 0 \\ 0 & e^{i\varphi} \end{pmatrix}$ , where  $\varphi$  is the phase shift. This is an essential operation in quantum Fourier transforms. We consider a representation of a logical phi-bit states in the form:  $\vec{U}'' = \begin{pmatrix} e^{i\varphi_{12}} \\ e^{i\varphi_{13}} \end{pmatrix}$ . We also consider four different phi-bits corresponding to nonlinear modes in the metamaterial Fourier spectrum with the frequencies: (phi-bit I)  $f_1 - 4\Delta f$ , (phi-bit II)  $2f_1 + f_2 - 4\Delta f$ , (phi-bit III)  $2f_1 + f_2 - 3\Delta f$  and (phi-bit IV)  $2f_1 + f_2 - 2\Delta f$ . Figures 3(a)–6(a) report the variation in phases  $\varphi_{12}$  and  $\varphi_{13}$  for the four phi-bits over the same range of tuning parameter. In all cases  $\varphi_{12}(\Delta v)$  varies only slightly compared to  $\varphi_{13}(\Delta v)$ . The components  $e^{i\varphi_{12}}$  and  $e^{i\varphi_{13}}$  are plotted in the complex plane with states represented on the unit circle. The four phi-bit approximate well the complete set of superpositions of states:  $\begin{pmatrix} -1 \\ e^{i\varphi_{13}(I)} \end{pmatrix}$ ,  $\begin{pmatrix} 1 \\ e^{i\varphi_{13}(II)} \end{pmatrix}$ ,  $\begin{pmatrix} i \\ e^{i\varphi_{13}(III)} \end{pmatrix}$ , and  $\begin{pmatrix} -i \\ e^{i\varphi_{13}(IV)} \end{pmatrix}$ . Note that the phi-bit state components are now complex quantities. By changing the tuning parameter, the first component remains constant to within some well characterized interval while the second component varies over a sizeable section of the unit circle. The complex plane could be completely spanned by the second component if one were to use another representation of the phi-bit states taking the form:  $\begin{pmatrix} e^{i\varphi_{12}} \\ e^{im\varphi_{13}} \end{pmatrix}$  where  $m$  is some coefficient introduced to rescale the phase  $\varphi_{13}$ .

The phase gate can then be applied physically by varying  $\Delta v$ .

### 3.3. Example algorithm with three phi-bits

So far, we have considered phi-bits and ranges of tuning parameter that were associated with monotonous variations in the phases  $\varphi_{12}$  and  $\varphi_{13}$ . As was shown in the sections 2, the complex amplitudes of phi-bit states are composed of products of resonant amplitudes. In figure 7, we show  $\pi$  jumps in the phases associated with such resonant processes for the phi-bits II, III, and IV.

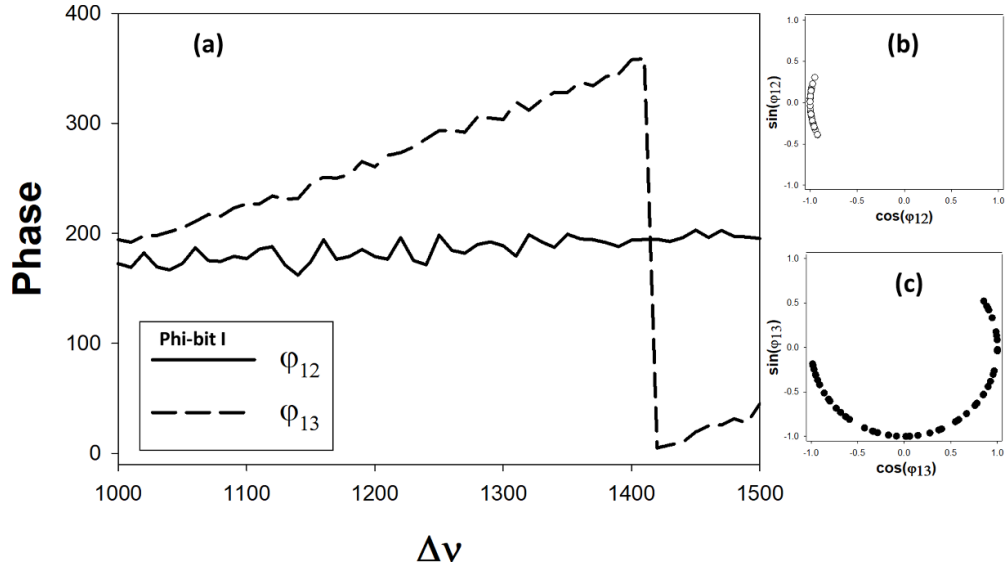


**Figure 3.** Phi-bit I with frequency  $f_1 - 4\Delta f$ . (a) Phases  $\varphi_{12}$  and  $\varphi_{13}$  as functions of driving frequency tuning parameter  $\Delta\nu$  over the range 1000–1500 Hz. (b) and (c) location of the components of the  $\tilde{U}''$  representation on the unit circle in the complex plane for the different values of the tuning parameter. The open and closed symbols correspond to the components  $e^{i\varphi_{12}}$  and  $e^{i\varphi_{13}}$ , respectively. The  $2\pi$  discontinuity is inconsequential.

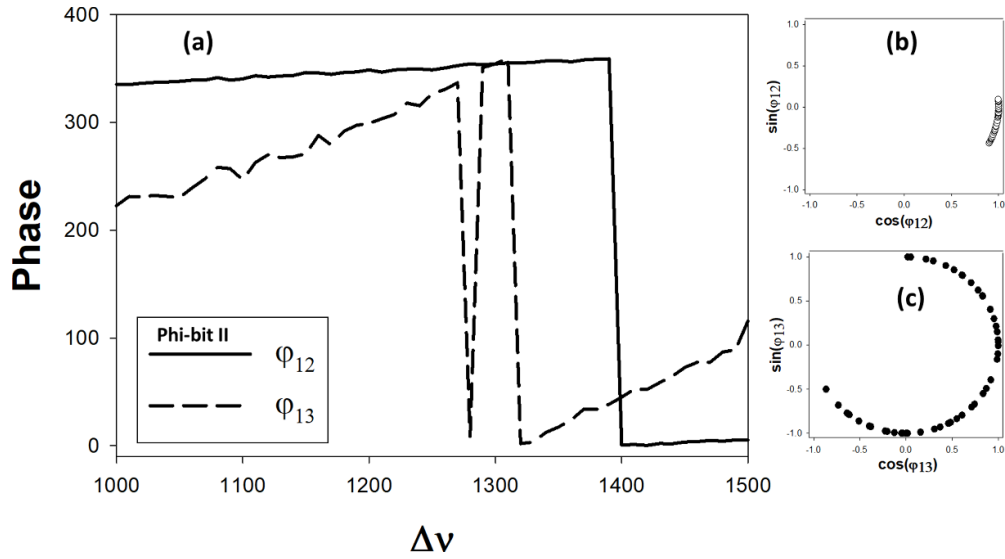


**Figure 4.** Same as figure 3 but for Phi-bit II with frequency  $2f_1 + f_2 - 4\Delta f$ . The  $2\pi$  discontinuities are inconsequential.

These resonances can be exploited to develop additional operations on phi-bits states via variations in  $\Delta\nu$ . We now treat the system of three phi-bits II, III, and IV as partitioned into a two phi-bit (III and IV) composite system and another reference phi-bit (II). The state of

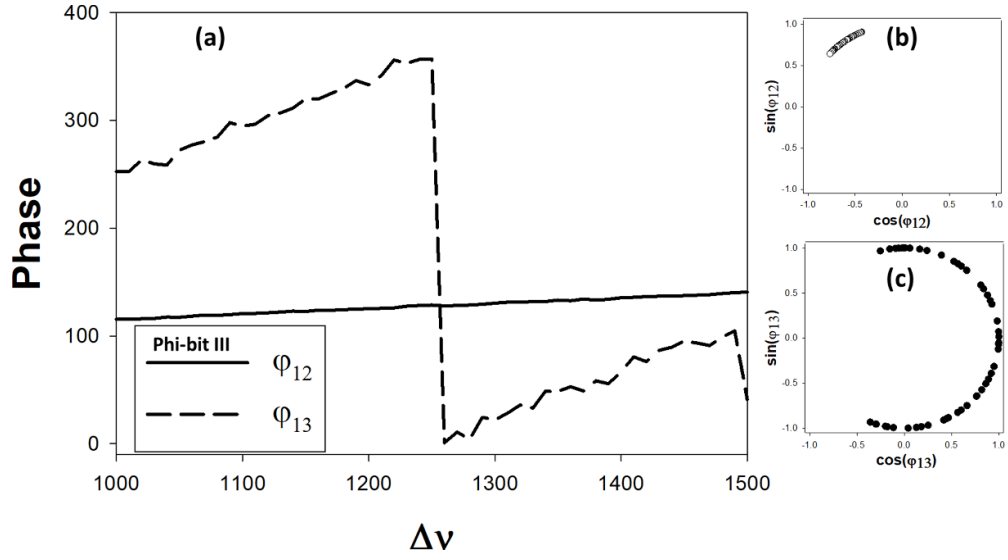


**Figure 5.** Same as figure 3 but for Phi-bit III with frequency  $2f_1 + f_2 - 3\Delta f$ .

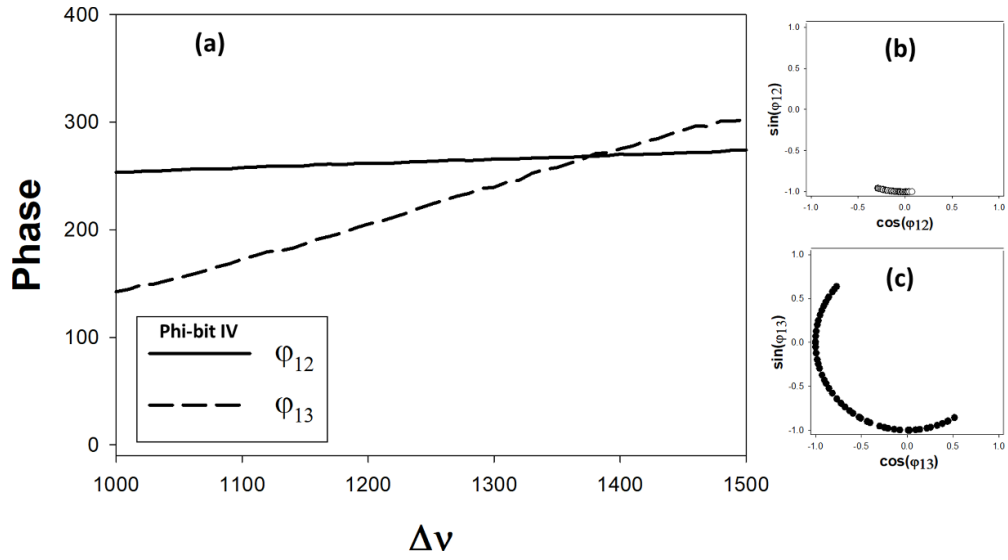


**Figure 6.** Same as figure 3 but for Phi-bit IV with frequency  $2f_1 + f_2 - 2\Delta f$ .

the two phi-bit composite evolves now in a  $2^2$ -dimensional Hilbert space while the state of the remaining phi-bit spans a two-dimensional space. We now employ a two phi-bit representation given by:

$$\vec{U}(III-IV) = \begin{pmatrix} 1 + e^{i(\varphi_{12}^*(III) + \varphi_{12}^*(IV))} \\ 1 + e^{i(\varphi_{12}^*(III) + \varphi_{13}^*(IV))} \\ 1 + e^{i(\varphi_{13}^*(III) + \varphi_{12}^*(IV))} \\ 1 + e^{i(\varphi_{13}^*(III) + \varphi_{13}^*(IV))} \end{pmatrix}. \quad (32)$$

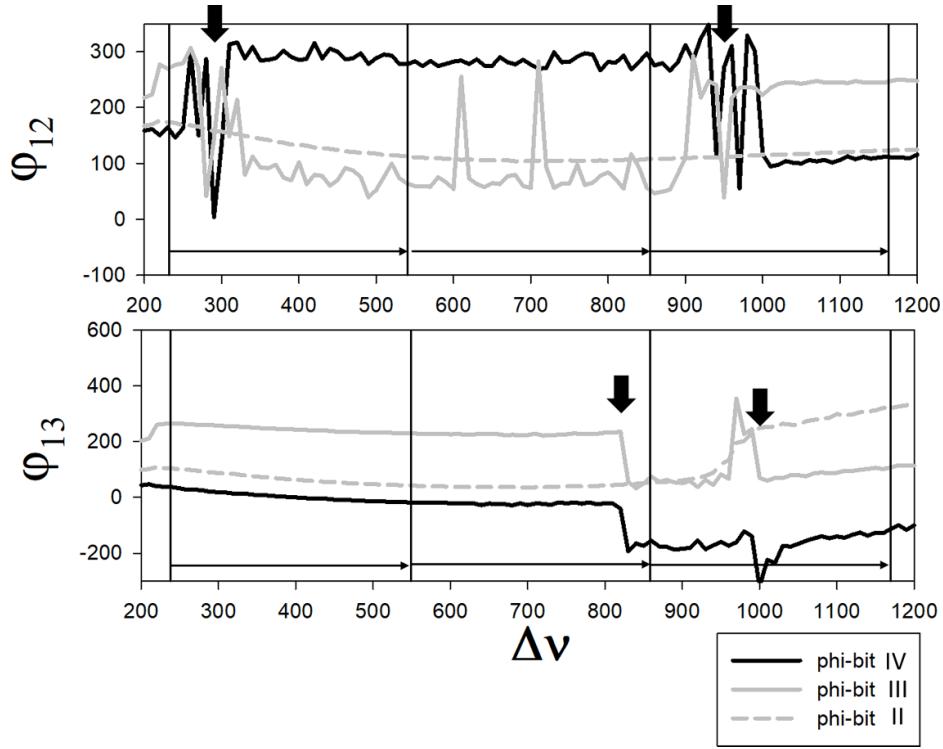


**Figure 7.** Phases  $\varphi_{12}$  and  $\varphi_{13}$  of phi-bits II, III, and IV as functions of driving frequency tuning parameter  $\Delta\nu$  over the range 200–1200 Hz. The large black arrows mark the location of  $\pi$  jumps in the phases. The equally spaced vertical lines indicate selected states of the three phi-bit system (see text for details). The experimental data includes inconsequential  $2\pi$  discontinuities as phases are defined modulo  $2\pi$ .

Since the phases  $\varphi_{12}$  and  $\varphi_{13}$  exhibit monotonous variations as well as resonant  $\pi$  jumps, in equation (32), the phases  $\varphi_{12}^*$  and  $\varphi_{13}^*$  are stripped from the monotonous variations and include only the resonant changes. Furthermore, all phases are translated to the origin at  $\Delta\nu = 200$  Hz. Figure 8 illustrates schematically this adjustment.

In this representation, the states of the III–IV composite are given in table 2.

Starting with a tuning parameter at  $\Delta\nu = 230$  Hz, the two phi-bit state alternates between

$\begin{pmatrix} 1 \\ 1 \\ 1 \\ 1 \end{pmatrix}$  and  $\begin{pmatrix} 1 \\ 0 \\ 0 \\ 1 \end{pmatrix}$  for every increment of the tuning parameter of 315 Hz. Effectively the

four-dimensional state vector follows a closed loops in the Hilbert space of the two phi-bit composite system. Note that the identical first and third states are separable into a tensor product of two individual phi-bit states, while the second and fourth states are non-separable. The matrix associated with the unitary operation that corresponds to the physical action of incrementing the tuning parameter is:

$$Q = \frac{1}{\sqrt{2}} \begin{pmatrix} 1 & 1 & 0 & 0 \\ 1 & -1 & 0 & 0 \\ 0 & 0 & -1 & 1 \\ 0 & 0 & 1 & 1 \end{pmatrix}.$$

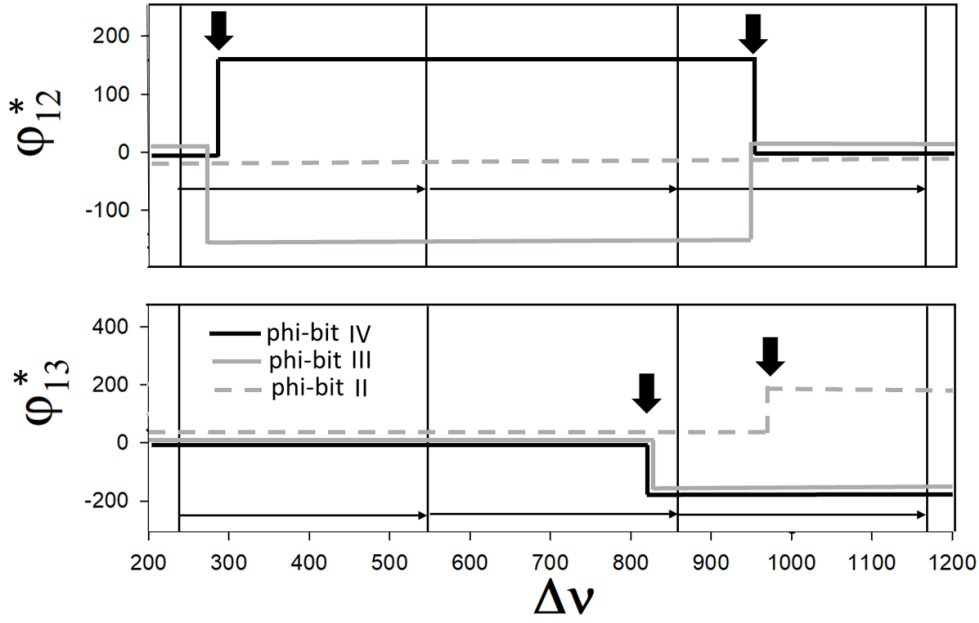


**Figure 8.** Same as figure 7. The solid black, solid gray and dashed gray curves represent the phases  $\varphi_{12}^*$  and  $\varphi_{13}^*$  adjusted to include only resonant variations with the tuning parameter.

**Table 2.** States of the two phi-bit III–IV composite system and the values of their corresponding tuning parameter. Note that the states in this table are to be normalized by  $\frac{1}{2}$  for the first and third states and  $\frac{1}{\sqrt{2}}$  for the second and fourth states.

$\Delta\nu(\text{Hz})$	230	545	860	1175
State	$\begin{pmatrix} 1 \\ 1 \\ 1 \\ 1 \end{pmatrix}$	$\begin{pmatrix} 1 \\ 0 \\ 0 \\ 1 \end{pmatrix}$	$\begin{pmatrix} 1 \\ 1 \\ 1 \\ 1 \end{pmatrix}$	$\begin{pmatrix} 1 \\ 0 \\ 0 \\ 1 \end{pmatrix}$

Note that this unitary transformation can be written as the combination of some of the more fundamental quantum gates:  $Q = -\sigma_z \otimes \sigma_z + \sigma_x \otimes I$  where  $\sigma_x$ ,  $\sigma_z$  and  $I$  are  $2 \times 2$  Pauli gates and identity matrix. This transformation can be used to develop algorithms. Let us consider

that we can go from a state  $\begin{pmatrix} 1 \\ 0 \\ 0 \\ 1 \end{pmatrix}$  starting at  $\Delta\nu = 545$  Hz to another identical state  $\begin{pmatrix} 1 \\ 0 \\ 0 \\ 1 \end{pmatrix}$

by two routes. The first route is to apply an operation associated with the  $4 \times 4$  identity matrix whereby one does not change  $\Delta\nu$ . The second route is to apply the matrix operation  $Q$  twice, that is, change  $\Delta\nu$  by adding  $2 \times 230$  Hz. In the first case the phi-bit II does not change its state.

For instance, using the representation  $\vec{U}(II) = \begin{pmatrix} 1 + e^{i\varphi_{12}^*(II)} \\ 1 + e^{i\varphi_{13}^*(II)} \end{pmatrix}$ , phi-bit II remains in the state  $\begin{pmatrix} 1 \\ 1 \end{pmatrix}$ . However, in the case of the second route, the state of phi-bit II changes to  $\begin{pmatrix} 1 \\ 0 \end{pmatrix}$ .



because we have crossed one of its resonant  $\pi$  jump. We can measure that change on phi-bit II while the state of the III–IV composite system has not effectively changed. This is a controlled operation. We can then develop an algorithm that can differentiate whether a function,  $f(X)$  of a single variable  $X \in [1, 2, 3, 4]$  is a constant, say 1, or is linear say  $f(X) = X$ . For this, we may redefine the matrix  $Q$  as follows:

$$Q_f = \frac{1}{\sqrt{2}} \frac{f(4)-f(3)+f(2)-f(1)}{2} \times \begin{pmatrix} (-1)^{1+f(1)} & \frac{1}{2} (1 + (-1)^{f(2)}) & 0 & 0 \\ \frac{1}{2} (1 + (-1)^{f(2)}) & (-1)^{1+f(2)} & \frac{1}{2} (1 + (-1)^{f(3)}) & 0 \\ 0 & \frac{1}{2} (1 + (-1)^{f(3)}) & (-1)^{1+f(4)} & \frac{1}{2} (1 + (-1)^{f(4)}) \\ 0 & 0 & \frac{1}{2} (1 + (-1)^{f(4)}) & (-1)^{1+f(3)} \end{pmatrix}$$

where  $Q_f$  realizes the identity matrix if the function  $f$  is constant and the unitary transformation  $Q$  if the function is linear. We can therefore identify the character of the function in one single iteration. The algorithm has the following steps. Initialize the system of three phi-bits at  $\Delta v = 545$  Hz. An oracle, i.e. an operation that is used as input to the algorithm, applies either no change in the tuning parameter if the function is constant or adds 460 Hz if the function is linear. The state of the two phi-bits III–IV does not change but one can read the output in the change of phase of phi-bit II. Phi-bits III and IV serve as control inputs (their state does not change) to the unitary gate  $Q_f$  which alters the phase of phi-bit II. Note that phi-bit II allows us to measure changes (or not) in the representation space of phi-bits III and IV. This provides access to the mathematical structure of a representation.

#### 4. Conclusions

The pursuit of digital quantum computers is in part a quest to power scientific discovery in materials modeling and simulation. However, quantum computers constituted of multiple qubits suffer from decoherence of quantum superpositions of states due to undesired interactions, imposing the development of cumbersome strategies for suppressing environmental effects [9, 10] and performing error corrections [11]. These strategies limit current simulations of materials to toy models. In contrast, here, we exploit analogies between quantum wave functions and classical acoustic waves in metamaterials, namely coherent superpositions of states that are robust against decoherence, to realize quantum-like gate operations that may serve as a resource to complement quantum systems in harnessing the power of complexity in quantum information processing and materials simulations. We exploit the strong coupling and nonlinearity of acoustic waves in metamaterials to develop the notion of correlated logical phi-bits. Indeed, in contrast to other types of waves such as optical waves, sound supporting media such as acoustic metamaterials offer a broader palette of nonlinear responses that may result from different type, strength and order of nonlinearity [12]. Phi-bits—classical analogues of qubits—offer new approaches to realize superpositions of states for classical multipartite systems that span exponentially complex Hilbert spaces. The properties of logical phi-bits parallel those of qubits from coherent superpositions to non-separability, to strong correlations. Quantum superpositions also exhibit the unique property of nonlocality, however, since logical phi-bits live in the spectral domain of the same physical metamaterial, there is no issue with their spatial separation. We show that we can operate upon superpositions of phi-bit states to achieve quantum-like gates in systematic, controllable, and predictable ways. Here, we demonstrate two single phi-bit gates, namely the Hadamard and the phase shift gates as well as a three

phi-bit controlled gate. While single phi-bit gates do not exploit the non-separability of classical waves and may be easily realizable in classical systems, the three phi-bit controlled gate demonstrated herein is associated with unitary operations that transforms separable multi phi-bit states into non-separable states (i.e. classically entangled states). These operations act on different representations of the complex phi-bit/multi phi-bit amplitude by rotating their vector states within the corresponding Hilbert space, thus accumulating a geometric phase. It has been proposed that the geometric phase can be used for enabling quantum computation [13]. Acoustic analogues of quantum systems provide easy to use classical physical platforms for testing or mimicking quantum behaviors [14, 15] offering avenue to use acoustic metamaterials for quantum computation [16]. Therefore, this paper sets the stage for the implementation of a set of universal quantum-like gates on an acoustic metamaterials digital quantum analogue computer that may enable simulation of materials beyond simple models.

### Data availability statement

The data that support the findings of this study are available upon reasonable request from the authors.

### Acknowledgments

This research was funded in part by the National Science Foundation Emerging Frontiers in Research and Innovation (EFRI) Award (No.1640860). The development of the metamaterial system and apparatus was supported in part by a grant from the W M Keck foundation. M A H thanks Wayne State University Startup funds for support.

### ORCID iDs

P A Deymier  <https://orcid.org/0000-0002-1088-7958>

M A Hasan  <https://orcid.org/0000-0001-7452-004X>

### References

- [1] Bassman L, Urbanek M, Metcalf M, Carter J, Kemper A F and de Jong W A 2021 Simulating quantum materials with digital quantum computers *Quantum Sci. Technol.* **6** 043002
- [2] Ma H, Govoni M and Galli G 2020 Quantum simulations of materials on near-term quantum computers *npj Comput. Mater.* **6** 85
- [3] Smith A, Kim M K, Pollmann F and Knolle J 2019 Simulating quantum many-body dynamics on a current digital quantum computer *npj Quantum Inf.* **5** 106
- [4] Jouzdani P and Bringuier S 2021 Hybrid quantum-classical eigensolver without variation or parametric gates *Quantum Rep.* **3** 137
- [5] Djordjevic I B 2021 *Quantum Information Processing, Quantum Computing, and Quantum Error Correction* 2nd edn (New York: Academic)
- [6] Johnson T H, Clark S R and Jaksch D 2014 What is a quantum simulator? *EPJ Quantum Technol.* **1** 10
- [7] Hasan M A, Runge K and Deymier P A 2021 Experimental classical entanglement in a 16 acoustic qubit-analogue *Sci. Rep.* **11** 24248
- [8] Runge K, Hasan M A, Levine J A and Deymier P A 2022 Demonstration of a two-bit controlled-NOT quantum-like gate using classical acoustic qubit-analogues *Sci. Rep.* **12** 14066
- [9] Rong X, Geng J, Shi F, Liu Y, Xu K, Ma W, Kong F, Jiang Z, Wu Y and Du J 2015 Experimental fault-tolerant universal quantum gates with solid-state spins under ambient conditions *Nat. Commun.* **6** 8748

- [10] Kandala A, Wei K X, Srinivasan S, Magesan E, Carnevale S, Keefe G A, Klaus D, Dial O and McKay D C 2021 Demonstration of a high-fidelity CNOT gate for fixed-frequency transmons with engineered ZZ suppression *Phys. Rev. Lett.* **127** 130501
- [11] Gottesman D 2002 *An Introduction to Quantum Error Correction*, in *Quantum Computation: A Grand Mathematical Challenge for the Twenty-First Century and the Millennium* ed S J Lomonaco Jr (Providence, RI: American Mathematical Society) pp 221–35
- [12] Deymier P A and Runge K 2017 *Sound Topology, Duality, Coherence and Wave-Mixing: An Introduction to the Emerging New Science of Sound* vol 188 (Berlin: Springer)
- [13] Sjöqvist E, Tong D M, Andersson L M, Hessmo B, Johansson M and Singh K 2012 Non-adiabatic holonomic quantum computation *New J. Phys.* **14** 103035
- [14] Tang S, Wu J-L, Lü C, Wang X, Song J and Jiang Y 2022 Acoustic wavelength-selected metamaterials designed by reversed fractional stimulated Raman adiabatic passage *Phys. Rev. B* **105** 104107
- [15] Shen Y-X, Peng Y-G, Zhao D-G, Chen X-C, Zhu J and Zhu X-F 2019 One-way localized adiabatic passage in an acoustic system *Phys. Rev. Lett.* **122** 094501
- [16] Xu G 2022 A bridge between acoustic metamaterials and quantum computation *Sci. China Phys. Mech. Astron.* **65** 220311